NIH Public Access
Author Manuscript
Retina. Author manuscript; available in PMC 2012 May 1.

Published in final edited form as:
Retina. 2011 May ; 31(5): 949–958. doi:10.1097/IAE.0b013e3181f441f6.

SLO-infrared imaging of the macula and its correlation with functional loss and structural changes in patients with Stargardt disease

Anastasios Anastasakis, MD[1], **Gerald A Fishman, MD**[1], **Martin Lindeman, COMT**[1], **Mohamed A Genead, MD**[1], and **Wensheng Zhou, MD**[2]

[1]Department of Ophthalmology and Visual Sciences, University of Illinois at Chicago, Chicago, IL

[2]OPKO Instrumentations, Miami, FL

Abstract

Purpose—To correlate the degree of functional loss with structural changes in patients with Stargardt disease.

Methods—Eighteen eyes of 10 Stargardt patients were studied. Scanning laser ophthalmoscope (SLO) infrared images were compared to corresponding spectral domain optical coherence tomography (SD-OCT) scans. Additionally, SLO microperimetry was performed and results were superimposed on SLO infrared images and in selected cases on fundus autofluorescence (FAF) images.

Results—Seventeen of 18 eyes showed a distinct hypo-reflective foveal and/or perifoveal area with distinct borders on SLO-infrared images which was less evident on funduscopy and incompletely depicted in FAF images. This hypo-reflective zone corresponded to areas of significantly elevated psychophysical thresholds on microperimetry testing, in addition to thinning of the retinal pigment epithelium (RPE), disorganization or loss of the photoreceptor cell inner-outer segment (IS-OS) junction and external limiting membrane (ELM) on SD-OCT.

Conclusion—SLO-infrared fundus images are useful for depicting retinal structural changes in Stargardt patients. An SD-OCT/SLO microperimetry device allows for a direct correlation of structural abnormalities with functional defects that will likely be applicable for the determination of retinal areas for potential improvement of retinal function in these patients during future clinical trials and for the monitoring of the diseases' natural history.

Keywords

microperimetry; SLO infrared imaging; Stargardt disease; fundus autofluorescence imaging

Correspondance: Dr. Gerald A Fishman Address: 1855 W. Taylor Street Suite 3.85 Chicago, IL 60612 USA Phone: +1 312 996 8939 Fax: + 1 312 996 1950 gerafish@uic.edu.

Author WZ is an employee of OPKO Instrumentation Incorporated. His current position is director of medical affairs. He personally has no OPKO stocks.

The authors (AA, GAF, ML, MAG) have no financial or proprietary interest in any of the products or techniques mentioned in this article.

This is a PDF file of an unedited manuscript that has been accepted for publication. As a service to our customers we are providing this early version of the manuscript. The manuscript will undergo copyediting, typesetting, and review of the resulting proof before it is published in its final citable form. Please note that during the production process errors may be discovered which could affect the content, and all legal disclaimers that apply to the journal pertain.

NIH-PA Author Manuscript
NIH-PA Author Manuscript
NIH-PA Author Manuscript

NIH-PA Author Manuscript

NIH-PA Author Manuscript

NIH-PA Author Manuscript

Introduction

Stargardt disease, first described in 1909 by Karl Stargardt,1 represents the most common form of juvenile onset, hereditary macular dystrophy that leads to progressive loss of (predominantly) central visual function. It is an autosomal recessive disease, affecting approximately 1 in 8000 to 1 in 10000 people in the United States.2 Mutations in the photoreceptor specific *ABCA4* gene can be identified in a significant percentage of cases.3 The hallmark of the disease is the presence of yellowish-white flecks in the macular region, or diffusely distributed in the fundus (according to the various stages of the disease), with or without an accompanying atrophic-appearing macular lesion.4

In diseases such as Stargardt disease, it is often difficult to determine the extent of macular impairment on the basis of ophthalmoscopic findings, especially in early stages when changes may be subtle, but also in more advanced stages when retinal pigment epithelium (RPE) and choriocapillaris atrophy can ensue. The correlation of ophthalmoscopic findings with fluorescein angiography (FA), infrared images and fundus autofluorescence (FAF) is useful, but additional correlation with functional impairment is also necessary for a more comprehensive evaluation of the patient.

Optical coherence tomography (OCT) is a non-invasive technique that has been used for detecting structural alterations in Stargardt patients.5-9 The development of spectral domain OCT (SD-OCT) combined with infrared SLO imaging made possible for the clinician an opportunity to simultaneously view high resolution cross sectional images of the retina and SLO infrared (surface) images for direct comparison of the retinal surface morphology with the architecture of various retinal layers. Furthermore, recent advances in OCT technology have combined the use of functional testing, such as microperimetry, with imaging modalities.

In the current study, we used SLO infrared imaging and SD-OCT for the assessment of structural alterations in Stargardt disease, and correlated structural changes with the degree of functional impairment.

Methods

Instruments and Techniques

SLO infrared images, OCT images and SLO microperimetry were performed using a commercially available SD-OCT/SLO combination imaging system (OPKO Instrumentation, Miami, FL). The SD-OCT/SLO is a high resolution tomographic and confocal imaging device. It is indicated for in vivo viewing of axial cross-sectional and three-dimensional images of posterior ocular structures. During the scanning mode, two images are simultaneously produced and displayed. One is a spectral domain OCT and the other is a confocal image of the fundus. It uses light generated from an infrared broadband super luminescent diode source with a central wavelength frequency of 830nm. As both the confocal fundus (retinal surface) image and the cross-sectional OCT images are generated through the same optics concurrently, they are displayed simultaneously on a computer screen and are pixel to pixel correspondent, so that direct correlations of the SLO infrared image with the OCT scan can be made.

Macular microperimetry was performed in patients who could maintain stable fixation (well defined retinal locus was identified) using the SD-OCT/SLO OPKO microperimeter software provided with the instrument. All tests were performed after mydriasis and the non-tested eye was always patched. The patients were instructed to fixate on a fixation target and to press a button when a flash of light was seen (Goldmann III size stimulus, 200ms stimulus

NIH-PA Author Manuscript

NIH-PA Author Manuscript

NIH-PA Author Manuscript

duration, test strategy 4-2). A customised grid pattern was created, according to the SLO infrared image, in patients with relatively large lesions so that all retinal areas of interest could be tested, while a standard grid (Polar 3) was used in one patient with a relatively small, well circumscribed lesion. A dense scotoma was considered to be present when even the brightest 0 dB stimulus (corresponding to 125 cd/m^2 higher than the luminous intensity from the background) was not seen. Subnormal responses were subdivided into markedly subnormal (4dB or less), moderately subnormal (6-10dB) and mildly subnormal (12-14dB) accordingly. Normal responses were considered when the dimmest stimuli (16-20dB) were seen. SLO microperimetry provides the advantage of viewing the retina while visual field testing (perimetry) is performed, so that a correlation of scotomas to observed lesions can be made directly, and so that a patient's fixation pattern can be identified and correction for eye movements by the instrument can be made.

FAF images were obtained in selected cases (patients 1-5, and 8) with a confocal scanning laser ophthalmoscope [(Retinal Angiograph (HRA) Heidelberg Engineering, Heidelberg, Germany]. The basic principles and technical characteristics of FAF testing have been described previously.[10, 11]

SLO microperimetry results projected onto infrared images were compared with the autofluorescence images by superimposing one on to the other and by side by side comparison. Because SLO microperimetry and FAF images were performed on different devices, for the overlaying procedure the lightbox software of the Spectral OCT/SLO system was utilized for superimposing microperimetry responses on the FAF images. The open source graphics program Gimp was used for comparison of the SLO infrared and FAF images. A transparent layer showing the outline of a lesion on an SLO infrared image was superimposed on the FAF image. Fundus photographs of each patient were also compared with SLO infrared and FAF images. Ten SLO infrared images and 10 FAF images of visually normal subjects (mean age was 35.4 years, range 26-59) were obtained for comparison with images from the patients.

Subjects

Ten patients (6 females, 4 males) with the diagnosis of Stargardt disease were included in the study after written informed consent was obtained. Explanations concerning the purpose of the study and the procedures to be used were provided to each patient. The study was conducted in accordance with the American Health Insurance Portability and Accountability Act (HIPAA) regulations and was approved by the Institutional Review Board of the University of Illinois at Chicago.

The diagnosis of Stargardt disease was established based on clinical presentation (funduscopic evidence of retinal flecks), presence of a dark choroid on FA and, in four patients, genetic testing. All patients underwent a full ophthalmic examination, including best corrected visual acuity, biomicroscopy, applanation tonometry, and fundoscopy. SLO imaging, SD-OCT, and microperimetry were performed as described above. Fundus reflectivity in SLO infrared images was defined as hyper-reflective when it appeared qualitatively increased in comparison to age-similar controls, as hypo-reflective when it appeared qualitatively decreased in comparison to the age-similar controls and as normally-reflective when it appeared of similar intensity to the age-similar controls. Furthermore, FAF images were obtained in selected cases, and 60° color fundus photographs were taken at the end of their examination in all patients. Blood samples were obtained on 5 patients for mutational screening of the *ABCA4* gene.

NIH-PA Author Manuscript

NIH-PA Author Manuscript

NIH-PA Author Manuscript

Results

Eighteen eyes of 10 patients were studied. Patient characteristics are shown in Table 1. Mean age (+/− S.D.) of the patients was 32.6 ±13 years (range 17-56). Best corrected visual acuity (BCVA) ranged from 20/20 to 20/400. Patients 2, 3, 4 and 6 had their causative mutations identified on the *ABCA4* gene. Data from microperimetry testing were utilizable in 15/18 eyes because patient 7 (OD) could not complete the test due to poor fixation and the responses from patient 2 (OU) did not cover the entire area that the macular lesion occupied on the SLO infrared image. Table 2 summarizes the findings from fundus photography, SLO infrared imaging and FAF imaging of the study population.

Funduscopic findings included either mild, mottled, hypo-pigmentary macular changes in four eyes of two patients, a bull's eye-appearing macular lesion (brownish-red area encircled by a hypopigmented area) in six eyes of four patients, or an atrophic (geographic) macular lesion observed in eight eyes of five patients. All 18 eyes included in this study showed abnormal changes in fundus reflectivity on SLO infrared imaging. Patients exhibiting a geographic, atrophic-appearing macular lesion, [patients 4-6(OU), and patients 7 and 9 (OD)], all showed a central, well circumscribed bright, hyper-reflective area that was partially or completely surrounded by a darker, annular hypo-reflective zone in 7/8 cases. Outside this zone, reflectance appeared similar to what was observed in control subjects. Geographic macular lesions appeared hyper-reflective centrally, on SLO infrared images most likely because of atrophic changes involving both the RPE and the choroidal vessels

Correlation of SLO infrared images with SD-OCT scans obtained in patients with geographic atrophy showed transverse loss of the photoreceptor IS-OS junction, ELM and thinning of the RPE, extending beyond the central hyper-reflective area, and corresponding well with the borders of the surrounding hypo-reflective zone. In one eye where the central hyper-reflective area was not surrounded by the hypo-reflective zone, correlation of the surface image (infrared) with the cross-sectional image showed that transverse loss of the photoreceptor IS-OS junction and ELM corresponded well with the outer border of the central hyper-reflective area.

Microperimetry responses superimposed on SLO infrared images (in 7/8 patients, since one could not complete the test due to poor fixation) were found to be 0dB or worse in the central hyper-reflective area of these patients with geographic macular atrophy, indicating the presence of a dense scotoma, while responses within the surrounding hypo-reflective zone ranged from 0db to 8db indicating markedly to moderately subnormal function. Fixation was found to be superior to the foveal region in all patients with an atrophic-appearing macular lesion.

Six eyes of four patients [patients 1 and 8 (OU), 9 (OS), and 10 (OD)], with a bull's eye-appearing macula lesion showed a normally-reflective region within the fovea surrounded by a hypo-reflective, dark area on SLO infrared imaging. In four eyes [patient 9(OS), 8 (OD),1(OU)], we additionally observed a centralised zone of hyper-reflectance within the normally-reflective foveal region. The size of the central normally-reflecting area varied from a small residual island (less than 1/4 of a disc diameter) to a well defined area (approximately 1/2 to 3/4 disc diameter). These hyper-reflective zones might be explained by either thinning of the RPE accompanied by choriocapillaris atrophy or by the enhanced accumulation of lipofuscin-like material. Correlations of SLO infrared images with SD-OCT scans in these patients with a bull's eye lesion, showed loss of the IS-OS junction of the photoreceptors, ELM and thinning of the RPE corresponding well with the hypo-reflective area on the SLO infrared images and preservation, to various degrees, of these retinal layers in the central normally-reflective area. Eyes with a bull's eye macular lesion had

NIH-PA Author Manuscript

NIH-PA Author Manuscript

NIH-PA Author Manuscript

microperimetry responses ranging from 4 to 16dB (indicating markedly subnormal to normal function) in the central normally-reflective area, while responses in the surrounding hypo-reflective area ranged from 0-12dB indicating markedly to mildly subnormal function. Outside the hypo-reflective zone, microperimetry responses ranged between moderately subnormal to normal (6-18 dB.). Fixation was found to be foveal in all six eyes of patients with a bull's eye-appearing macular lesion.

Four eyes of patients 2 and 3 with mild, mottled, hypopigmentary macular changes on fundus photographs showed a central foveal hypo-reflective area on SLO infrared imaging, while surrounding retinal reflectivity appeared to be similar to age-similar controls. Correlation of the SLO infrared images with the SD-OCT scans in these four eyes showed disorganisation and loss of the photoreceptor IS-OS junction and ELM while the RPE did not appear thinned. These changes on SD-OCT corresponded to the zone of hypo-reflectance on infrared images. Microperimetry thresholds superimposed on SLO infrared images ranged from 0 dB to 6 dB in the hypo-reflective central foveal area. As previously noted, microperimetry responses obtained from the two eyes of patient 2 were excluded. Fixation was found to be superior to the foveal zone in all 4 eyes with mottled hypopigmentary changes of the macula.

FAF images obtained in 12 eyes showed a perifoveal ring of enhanced FAF in 10 eyes. This was surrounding an area of either mottled foveal loss of FAF or normal foveal autofluorescence. Of the 10 eyes with enhanced perifoveal FAF, four eyes showed a bull's eye macular lesion, two eyes showed a small geographic, atrophic-appearing macular lesion and four eyes showed mottled hypopigmentary changes on fundus photographs. The two eyes that did not show an enhanced perifoveal ring of FAF, (patient 5) showed a central area of loss in FAF, corresponding to the atrophic macular lesion on fundus photographs that was surrounded by an area of patchy loss of FAF. All eyes (12) that underwent FAF showed focal areas of increased FAF in the posterior pole corresponding to the fundus flecks seen clinically. Superimposing microperimetry responses to FAF abnormalities showed that retinal sensitivity within the enhanced ring of FAF was markedly decreased (less than 4 dB) in four eyes while six eyes had markedly to moderately subnormal responses in this zone (0-10dB).

Functional and structural correlations in a patient exhibiting a geographic, atrophic-appearing macular lesion

Figure 1, A, B and C shows the fundus photograph, SLO infrared image and FAF image respectively, from the right eye of a 56-year-old woman (patient 5, Tables 1 and 2) with Stargardt disease. Visual acuity was 20/200. A previously obtained FA showed the presence of a dark choroid. The fundus photograph (A) showed a geographic atrophic-appearing macular lesion with small clumps of pigment surrounded by a ring of yellowish-white flecks. An SLO infrared image (B) showed a central, bright, hyper-reflective area, which corresponded to the atrophic macular lesion surrounded by a darker, hypo-reflective zone with distinct borders. The hypo-reflective zone is consistent with an area where there is thinning and hypopigmentation of the RPE resulting in absorption of the infrared light by the underlying choriocapillaris. FAF imaging (C) showed a central black area with total loss of autofluorescence surrounded by grayish-black patchy area which showed a mottled loss of FAF with poorly defined borders from the surrounding retina. The thin white line on Figure 1D represents the outer border of the hypo-reflective area on the SLO infrared image overlaid on the FAF image. This figure highlights that the SLO image displays more retinal structural alterations than the FAF image.

NIH-PA Author Manuscript

NIH-PA Author Manuscript

NIH-PA Author Manuscript

Superimposing microperimetry results on the SLO infrared image, (Figure 1E) showed that the hypo-reflective zone contains areas of moderately (8dB) and markedly (0-4dB) subnormal responses representing severely decreased but mostly detectable function. Fixation was not observed within this zone, but rather superonasally (small gray crosses) to the foveal region. Sensitivity outside this hypo-reflective area ranged between moderately (6-10dB) to mildly subnormal (12-14dB) responses. Similar correlation between FAF and microperimetry showed an area of non-detectable function corresponding to the black area of absent FAF, and an area of subnormal function within the poorly defined area of mottled loss of FAF.

Functional and structural correlations in a patient exhibiting a bull's eye macular lesion

Figure 2, A, B and C shows a fundus photograph, SLO infrared and FAF image respectively, from the right eye of a 27-year-old Stargardt patient (patient 1, Tables 1 and 2). Visual acuity of this eye was 20/20. The fundus photograph shows a bull's eye-appearing macular lesion surrounded by a ring of flecks with a normal-appearing optic disc and retinal vessels. The SLO infrared image shows a nummular shaped, normally reflecting foveal area with a central hyper-reflective patch within it (black arrow on Figure 2B). This foveal area is surrounded by a dark annular hypo-reflective zone where retinal pigment epithelial thinning and hypopigmentation permits the infrared light to be absorbed by the underlying choriocapillaris resulting in reduced reflectance. Autofluorescence imaging of the same patient shows a ring of patchy, mottled increase and speckled decrease in FAF around the fovea. Visualization of fundus flecks is significantly enhanced on the FAF image in comparison to the fundus photograph. Microperimetry testing showed either a dense (absolute) scotoma or markedly elevated thresholds present in the hypo-reflective dark area (Figure 2D). Fixation was foveal (small gray dots) and corresponding microperimetry responses within the fixation area were found to be in the range of mildly subnormal (14dB) to moderately subnormal (10dB). Figure 2E shows microperimetry responses superimposed on the FAF image of this patient. Retinal sensitivities were notably decreased in the region of enhanced AF, while sensitivities were less decreased in the central fovea and in areas of normal FAF.

Correlations of findings from cross sectional images and surface images

Comparison of the SLO infrared images with SD-OCT scans showed that in 17 eyes the dark hypo-reflective area marks the presence of loss in the IS-OS junction, ELM, and thinning of the RPE. Figure 3 (A, B) shows the SD-OCT scans of patients 5 and 1 juxtaposed over the area of the SLO infrared image where the scan was acquired and Figure 3C the corresponding image from a normally sighted control subject. Retinal structure in the fovea of patient 5 with geographic atrophy of the macula showed evidence of transverse loss of the ELM and photoreceptor IS-OS junction throughout the extent of the lesion as seen in Figure 3A. The disruption of the IS-OS junction (arrowhead) is accompanied by thinning and irregularity of the RPE. Brackets with arrowheads enclose the central foveal area where significant RPE thinning and hypopigmentation in addition to atrophy of the underlying choriocapillaris results in highly reflected infrared light (most probably from the sclera) and the bright appearance of the geographic-atrophic macular lesion on the SLO infrared image.

Comparison of the cross-sectional image with the surface image in Figure 3A shows that the central hyper-reflective area on the SLO infrared image corresponds well with the area of RPE atrophy, while the adjacent hypo-reflective, darker zone corresponds with the area of loss in the ELM, photoreceptor IS-OS junction and thinning of the RPE. Retinal layer architecture outside this region appears within normal limits.

NIH-PA Author Manuscript

NIH-PA Author Manuscript

NIH-PA Author Manuscript

Figure 3B shows a three dimensional image combining the SD-OCT scan and SLO infrared image from patient 1 with a bull's eye macular lesion. The foveal region on the SLO infrared image appears normally-reflective with the exception of a hyper-reflective center, conceivably due to accumulation of an increased amount of lipofuscin-like material in both the outer retina and RPE. The RPE-photoreceptor complex, IS-OS junction and ELM appear thickened and brighter (white arrow) in the fovea in comparison to the perifoveal region on the cross sectional image. This observation seems to correlate well with a previously published finding from an ultrahigh resolution OCT study12 where the authors attributed this enhanced reflectivity and increased thickness of the retinal layers in the foveal region to an increased accumulation of an auto-fluorescent substance. The dark hypo-reflective area encircling the fovea in the SLO infrared image corresponds well with the loss and disorganization of the photoreceptor IS-OS junction and ELM on SD-OCT scans.

Discussion

The current study used imaging techniques (SLO infrared, FAF and SD-OCT) in combination with SLO microperimetry to demonstrate changes in macular morphology and function in Stargardt patients. We evaluated patients with macular lesions that ranged from a bull's eye maculopathy, to a more advanced central macular lesion (geographic atrophy). Seventeen out of the 18 eyes in our study showed a distinct darker (hypo-reflective) zone of varying size on SLO infrared imaging that represented areas of outer retinal degeneration including either thinning or loss of RPE cells. These hypo-reflective regions do not simply represent hypopigmented RPE cells but rather signify areas of reduced visual function. They appear as hypopigmented changes on fundus exam that are more readily delineated on SLO infrared imaging.

Our findings on SLO infrared fundus imaging can likely be explained by the properties of infrared light,13,14 which penetrates into retinal and choroidal structures and allows visualization of deeper retinal layers. Intact RPE can absorb but mostly reflects infrared light, while hypopigmented and thinned RPE permits the penetration of infrared light that is absorbed by oxygen in the blood-filled choroidal vessels that results in a hypo-reflectance on infrared imaging.

This finding was demonstrated in a previous study15 where the authors compared SLO images in Stargardt patients, at 488 nm, 514nm, 633nm and 780nm and found that SLO images at the infrared spectrum showed more retinal abnormalities than blue light and concluded that infrared light is a sensitive monitor of early fundus changes in patients with Stargardt macular dystrophy.

Correlations of SD-OCT scans with SLO infrared images showed that abnormalities appearing on SLO infrared images (in terms of hypo-reflectance) correspond well with the loss of the IS-OS junction, ELM and thinning of the RPE in 17 out of 18 eyes that showed a hypo-reflective area. Thus, photoreceptor cell layer structural changes were accompanied by pigmentary changes at the level of the RPE. However, in some instances, thickness of the RPE layer had an almost normal structural appearance on OCT scans when the outer retinal layers were already disrupted as noted in four eyes from two patients. Cross sectional anatomical changes (observed on OCT scans) were associated with surface imaging changes on SLO infrared images as demonstrated on a three-dimensional image comparison. This comparison had significant clinical value for determining the extent of retinal impairment in our cohort but required optimal alignment of the patient during the scanning mode. Additionally, all patients in our study exhibiting abnormalities on SLO infrared images and distinct structural abnormalities on SD-OCT had corresponding significantly elevated thresholds on microperimetry testing.

NIH-PA Author Manuscript

NIH-PA Author Manuscript

NIH-PA Author Manuscript

In a recent study by Gomez and coworkers,16 the authors compared structural changes seen on SD-OCT to changes visible on FAF in 22 eyes from 11 patients with Stargardt disease. They demonstrated (in six eyes) that FAF may appear normal or show minor changes in the initial phase of the disease when structural changes are already present on SD-OCT testing. Furthermore, the authors reported that the diameter of abnormal FAF more closely approximated the loss in IS-OS junction in comparison to the area of absent FAF.16 Other investigators have also highlighted that the level of FAF in the macular region of Stargardt patients can be normal, despite abnormalities that are already present on SLO images and when abnormalities of macular function are present on pattern ERG testing.17 The most frequently observed lesion on FAF images in our study was a perifoveal, annular area of enhanced FAF (10/12 eyes) that accompanied a bull's eye-appearing macular lesion in four eyes, a small central atrophic appearing macular lesion in two eyes and mottled hypopigmentary macularlesionin four eyes, respectively. Although FAF imaging is useful for detecting abnormal accumulation of autofluorescent material such as lipofuscin (which plays a central role in the pathophysiology of Stargardt disease), the interpretation of these images may present certain difficulties. Abnormal FAF signals can derive either from a change in the amount of lipofuscin in the RPE cell cytoplasm or from the presence of autofluorescent material anterior to the RPE (photoreceptor outer segments).11 Hence, an abnormal FAF signal indicates a disease process but does not, necessarily, accurately provide information that can discriminate whether a defect has occurred at the level of the RPE or the photoreceptor cell layer.

Functional and structural correlations have been reported in terms of FAF and microperimetry. In a recent study18 where FAF images of 32 Stargardt patients were correlated with microperimetry in order to assess a retinal structural and functional correlation, the authors reported that areas of either a mottled loss or increase in autofluorescence did not adequately define non-functioning retinal regions. Other authors also agree that patchy areas of decreased or increased FAF are difficult to interpret, since they may or may not correspond to areas of measurable retinal function.19 When we compared microperimetry responses to FAF abnormalities, retinal sensitivity in the enhanced ring of FAF was markedly decreased in four eyes while six eyes had markedly to moderately subnormal responses. On the other hand, FAF images in our study showed that visualization of fundus flecks (especially newly formed flecks) was enhanced in comparison to SLO infrared images and fundus photographs. Overall comparison of imaging techniques showed that SLO infrared images detected a larger area of retinal pigmentary abnormalities that were less apparent on FAF images or fundus photographs (both in early and advanced cases).

In summary, a combined spectral domain OCT/SLO-microperimetry device allows direct correlations of structural abnormalities with functional defects that should be useful for monitoring patients but also for the determination of the most optimal retinal areas for potential improvement of retinal function in Stargardt patients during future clinical trials. Our study emphasizes that findings on SLO infrared testing can correlate with structural fundus changes as determined by OCT testing, and the degree of functional loss, as measured by SLO-microperimetry, in both early and advanced stages of disease in Stargardt patients and likely in patients with other inherited macular dystrophies.

Brief summary

A combined Spectral domain OCT/SLO-microperimetry device was shown to provide an opportunity to correlate structural abnormalities with the degree of functional impairment in patients with Stargardt disease.

NIH-PA Author Manuscript

NIH-PA Author Manuscript

NIH-PA Author Manuscript

Acknowledgments

Supported by the Foundation Fighting Blindness, Owing Mills, Maryland, and Grant Healthcare Foundation, Chicago, Illinois (GAF); NIH core grant EY01792; and an unrestricted departmental grant from Research to Prevent Blindness.

References

1. Stargardt K. Uber familiare progressive degeneration in der makulagegend des auges. Albrecht von Graefes Arch Klin Ophthalmol. 1909; 71:534–550.
2. Blacharski, PA. Fundus flavimaculatus. In: Newsome, DA., editor. Retinal dystrophies and Degenerations. Raven Press; New York: 1988. p. 135-159.
3. Westerfeld C, Mukai S. Stargardt's disease and the *ABCA4* gene. Seminars Ophthalmol. 2008; 23:59–65.
4. Fishman GA. Fundus flavimaculatus. A clinical classification. Arch Ophthalmol. 1976; 94:2061–2067. [PubMed: 999551]
5. Ergun E, Hermann B, Wirtitsch M, et al. Assessment of central visual function in Stargardt Disease/ Fundus Flavimaculatus with Ultrahigh-Resolution Optical Coherence Tomography. Invest Ophthalmol & Vis Sci. 2005; 46:310–316. [PubMed: 15623790]
6. Berisha F, Feke GT, Aliyeva S, et al. Evaluation of macular abnormalities in Stargardts disease using optical coherence tomography and scanning laser ophthalmoscope microperimetry. Graefes Arch Clin Exp Ophthalmol. 2009; 247:303–309. [PubMed: 18941768]
7. Querques G, Leveziel N, Benhamou N, Voigt M, Soubrane G, Souied EH. Analysis of retinal flecks in fundus flavimaculatus using optical coherence tomography. Br J Ophthalmol. 2006; 90:1157–1162. [PubMed: 16754647]
8. Querques G, Prato R, Iaculli C, et al. Correlation of visual function impairment and OCT findings in patients with Stargardt disease and fundus flavimaculatus. Eur J Ophthalmol. 2008; 18(2):239–247. [PubMed: 18320517]
9. Gerth C, Zawadzki RJ, Choi SS, Keltner JL, Park SS, Werner JS. Visualisation of lipofuscin accumulation in Stargardt macular dystrophy by High-Resolution Fourier-Domain Optical Coherence Tomography. Arch Ophthalmol. 2007; 125:575. [PubMed: 17420386]
10. Hassenstein A, Meyer CH. Clinical use and research applications of Heidelberg retinal angiography and spectral-domain optical coherence tomography- a review. Clin Exp Ophthalmol. 2009; 37:130–143.
11. Schmitz-Valckenberg S, Holz FG, Bird AC, Spaide RF. Fundus Autofluorescence Imaging. Review and Perspectives. Retina. 2008; 28:385–409. [PubMed: 18327131]
12. Wirtitsch MG, Ergun E, Hermann B, et al. Ultrahigh Resolution Optical Coherence Tomography in macular dystrophy. Am J Ophthalmol. 2005; 140(6):976–983. [PubMed: 16376639]
13. Elsner AE, Burns SA, Weiter JJ, Delori FC. Infrared imaging of subretinal structures in the human ocular fundus. Vis Research. 1996; 36:191–205.
14. Manivannan A, Kirkpatrick JNP, Sharp PF, Forrester JV. Clinical investigation of an infrared Digital scanning laser ophthalmoscope. Br J Ophthalmol. 1994; 78:84–90. [PubMed: 8123631]
15. Zhang X, Hargitai J, Tammur J, et al. Macular pigment and visual acuity in Stargardt macular dystrophy. Graefe's Arch Clin Exp Ophthalmol. 2002; 240:802–809. [PubMed: 12397427]
16. Gomez NL, Greenstein VC, Carlson JN, et al. A comparison of fundus autofluorescence and retinal structure in patients with Stargardt disease. Invest Ophthalmol Vis Sci. 2009; 50(8):3953–3959. [PubMed: 19324865]
17. Lois N, Halfyard AS, Bird AC, Holder GE, Fitzke FW. Fundus autofluorescence in Stargardt macular dystrophy-fundus flavimaculatus. Am J Ophthalmol. 2004; 138(1):55–63. [PubMed: 15234282]
18. Sunness JS, Steiner JN. Retinal function and loss of autofluorescence in Stargardt disease. Retina. 2008; 28:794–800. [PubMed: 18536594]
19. Sunness JS, Ziegler MD, Applegate CA. Issues in quantifying atrophic macular disease using retinal autofluorescence. Retina. 2006; 26:666–672. [PubMed: 16829810]

NIH-PA Author Manuscript

NIH-PA Author Manuscript

NIH-PA Author Manuscript

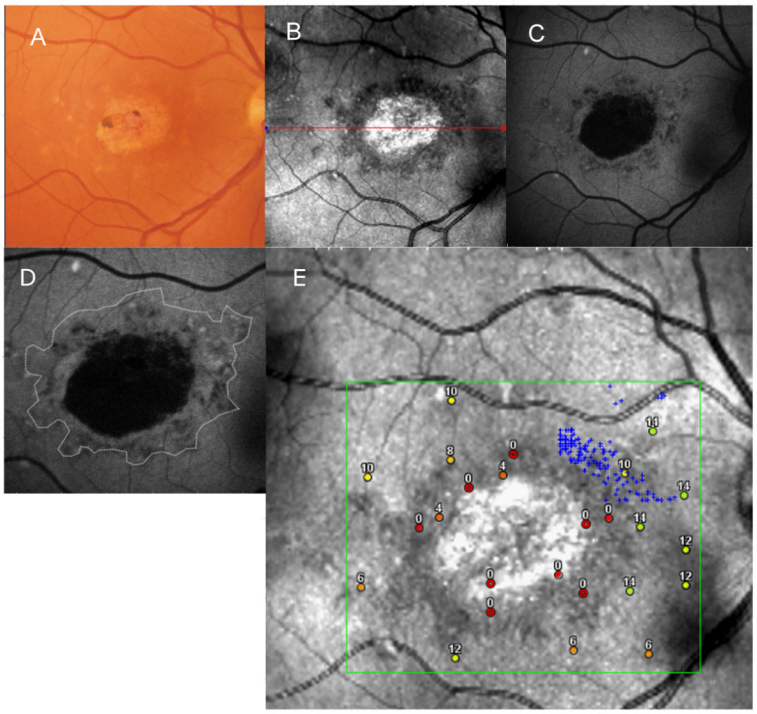

FIGURE 1.

(A, B, C) Composite of a color fundus photograph (gray scale), and SLO infrared and FAF images from patient 5 with a geographic, atrophic-appearing macular lesion.

(D) An outline of the atrophic macular lesion on SLO infrared imaging of patient 5, superimposed on the FAF image of this patient.

(E) Microperimetry responses superimposed on the SLO infrared image of patient 5.

NIH-PA Author Manuscript
NIH-PA Author Manuscript
NIH-PA Author Manuscript

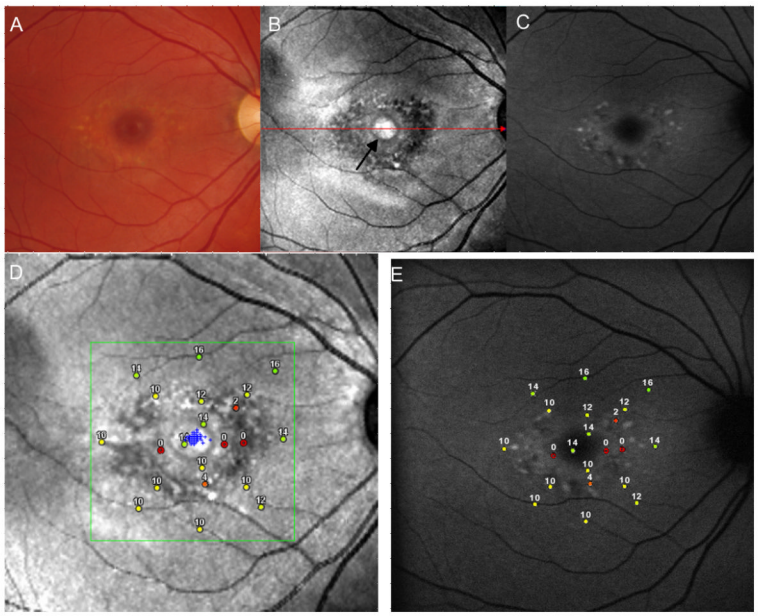

FIGURE 2.

(A, B, C): Composite of a color fundus photograph (gray scale) and SLO infrared and FAF images from patient 1 with a bull's eye-appearing macular lesion.

(D and E) Microperimetry responses of patient 1, superimposed on an SLO infrared image (D), and on an FAF image (E).

NIH-PA Author Manuscript
NIH-PA Author Manuscript
NIH-PA Author Manuscript

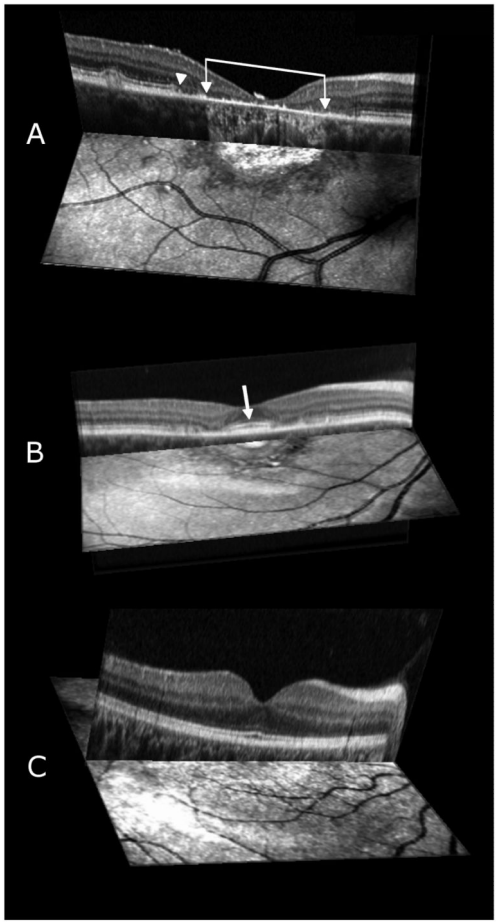

FIGURE 3.
(A, B, C) Three-dimensional images composed of an SD-OCT scan and a corresponding SLO infrared image of patient 5 with a geographic atrophic macular lesion (A), and patient 1 with a bull's eye-appearing macular lesion (B), and corresponding image from a control subject (C) respectively. Brackets with arrowheads enclose the atrophic macular lesion and white arrowhead shows the disruption of the IS-OS junction of the photoreceptors and ELM from patient 5 (Figure 3A). The white arrow on Figure 3B shows the increased thickness and brightness of the IS-OS junction of the photoreceptors in the foveal region of patient 1.

NIH-PA Author Manuscript NIH-PA Author Manuscript NIH-PA Author Manuscript

Retina. Author manuscript; available in PMC 2012 May 1.

Table1

The demographics of the patients, visual acuity and evidence upon the diagnosis was based are summarized.

Patient No. gender(M/F)*	Age	Race	Study Eye	BCVA	Diagnosis based upon: (*ABCA4* mutations identified)
1 - (F)	27	Caucasian	OD OS	20/20 20/20	Typical fundus changes
2 - (M)	17	Caucasian	OD OS	20/40 20/40	Typical fundus changes, dark choroid on FA** *(Gly863Ala)*
3 - (M)	30	Caucasian	OD OS	20/30 20/100	Typical fundus changes *(Arg1898his & Lys2056stop)*
4 - (F)	22	Caucasian	OD OS	20/200 20/200	Typical fundus changes, dark choroid on FA** *(Leu514Pro & Ala1038Val)*
5 - (F)	56	Caucasian	OD OS	20/200 20/200	Typical fundus changes, dark choroid on FA**
6 - (F)	40	Caucasian	OD OS	20/100 20/100	Typical fundus changes *(Gly1961Glu & Gly65Glu)*
7 - (M)	21	Caucasian	OD	20/300	Typical fundus changes
8 - (M)	36	African-American	OD OS	20/200 20/60	Typical fundus changes, dark choroid on FA**
9 - (F)	51	Caucasian	OD OS	20/400 20/30	Typical fundus changes, dark choroid on FA**
10 - (F)	26	Caucasian	OD	20/40	Typical fundus changes, family history of Stargart disease

*M = male, F = female

**FA = fluorescein angiography

NIH-PA Author Manuscript
NIH-PA Author Manuscript
NIH-PA Author Manuscript

Table 2

Summary of the findings on fundus photographs, SLO infrared images and fundus autofluorescence (FAF) images.

Patient Number / Eye	Color fundus photographs	SLO Infrared	FAF
1 – (OU*)	Bilateral bull's eye lesion macular lesion.	Central normally reflective area, surrounded by hypo-reflective zone (OU*).	Perifoveal ring of mottled hyper-autofluorescence surrounding normal foveal FAF (OU*).
2 – (OU*)	Bilateral, hypopigmentary changes in fovea.	Small foveal hypo-reflective area surrounded by normally reflective area (OU*).	Perifoveal ring of enhanced FAF (OU*).
3 – (OU*)	Bilateral, hypopigmentary changes in fovea.	Hypo-reflective foveal area surrounded by normally reflective area (OU*).	Non-specific mottled loss of foveal FAF, hyper-autofluorescence of fundus flecks (OU*).
4 – (OU*)	Small atrophic, geographic, macular lesion.	Hyper-reflective foveal area, surrounded by hypo-reflective area (OU*).	Foveal, lacy, annular pattern of enhanced FAF (OU*).
5 – (OU*)	Geographic, atrophic-appearing macular lesion.	Central hyper-reflective area, surrounded by hypo-reflective zone (OU*).	Central area of absent FAF, surrounded, by zone of mottled loss of FAF (OU*).
6 - (OU*)	Geographic atrophic appearing macular lesion.	Central hyper-reflective area, surrounded by hypo-reflective zone (OU*).	n. a.‡
7 - (OD†)	Geographic, atrophic-appearing macular lesion.	Central hyper-reflective area, without surrounding hypo-reflective zone.	n. a.‡
8 - (OU*)	Bilateral bull's eye macular lesion.	Normally reflective foveal area surrounded by hyper and hypo-reflective area (OU*).	Perifoveal ring of enhanced FAF surrounding foveal hypo-autofluorescence (OU*)
9 - (OU*)	OD†: Geographic, atrophic macular lesion. OS‡ Bull's eye macular lesion.	Central hyper-reflective area, partially surrounded by hypo-reflective zone normally reflective foveal area surrounded by hyper-reflective area	n. a.‡
10 - (OD†)	Bull's eye macular lesion.	Normally reflective small foveal area surrounded by hypo-reflective area.	n. a.‡

*both eyes

‡not available

†right eye

‡left eye